

An Efficient Framework for Whole-Page Reranking via Single-Modal Supervision

Zishuai Zhang

School of Artificial Intelligence,
Beihang University
Beijing, China
zhangzishuai@buaa.edu.cn

Ying Nie

Baidu Inc.
Beijing, China
niezengyings@gmail.com

Dawei Yin

Baidu Inc.
Beijing, China
yindawei@acm.org

Sihao Yu*

Baidu Inc.
Beijing, China
yush93@qq.com

Wenyi Xie

Baidu Inc.
Beijing, China
xiewenyi@baidu.com

Junfeng Wang

Baidu Inc.
Beijing, China
junfengzju@163.com

Zhiming Zheng

School of Artificial Intelligence,
Beihang University
Beijing, China
zhengzhiming0130@163.com

Hainan Zhang†

School of Artificial Intelligence,
Beihang University
Beijing, China
zhanghainan@buaa.edu.cn

Abstract

The whole-page reranking plays a critical role in shaping the user experience of search engines, which integrates retrieval results from multiple modalities, such as documents, images, videos, and LLM outputs. Existing methods mainly rely on large-scale human-annotated data, which is costly to obtain and time-consuming. This is because whole-page annotation is far more complex than single-modal: it requires assessing the entire result page while accounting for cross-modal relevance differences. Thus, how to improve whole-page reranking performance while reducing annotation costs is still a key challenge in optimizing search engine result pages(SERP). In this paper, we propose SMAR, a novel whole-page reranking framework that leverages strong Single-modal rankers to guide Modal-wise relevance Alignment for effective Reranking, using only limited whole-page annotation to outperform fully-annotated reranking models. Specifically, high-quality single-modal rankers are first trained on data specific to their respective modalities. Then, for each query, we select a subset of their outputs to construct candidate pages and perform human annotation at the page level. Finally, we train the whole-page reranker using these limited annotations and enforcing consistency with single-modal preferences to maintain ranking quality within each modality. Experiments on the

Qilin and Baidu datasets demonstrate that SMAR reduces annotation costs by about 70-90% while achieving significant ranking improvements compared to baselines. Further offline and online A/B testing on Baidu APPs also shows notable gains in standard ranking metrics as well as user experience indicators, fully validating the effectiveness and practical value of our approach in real-world search scenarios.

CCS Concepts

• **Information systems** → Rank aggregation; Learning to rank; Web search engines.

Keywords

Information Retrieval, Ranking, Relevance, Whole-Page Reranking

ACM Reference Format:

Zishuai Zhang, Sihao Yu, Wenyi Xie, Ying Nie, Junfeng Wang, Zhiming Zheng, Dawei Yin, and Hainan Zhang. 2018. An Efficient Framework for Whole-Page Reranking via Single-Modal Supervision. In *Proceedings of Make sure to enter the correct conference title from your rights confirmation email (Conference acronym 'XX)*. ACM, New York, NY, USA, 12 pages. <https://doi.org/XXXXXX.XXXXXXX>

1 Introduction

Search engines have evolved from simple document retrieval systems into complex platforms that must seamlessly integrate information across multiple modalities, including text, images, videos, and large language model(LLM) outputs [18, 21]. A central component of this process is whole-page reranking [12], which determines the final ordering and presentation of heterogeneous results on the search engine results page (SERP). As shown in Figure 1, the SERP contains various components corresponding to the user’s query. Unlike single-modal ranking, whole-page reranking requires balancing diverse signals of relevance, consistency, and user satisfaction.

*Corresponding author

†Corresponding author

Permission to make digital or hard copies of all or part of this work for personal or classroom use is granted without fee provided that copies are not made or distributed for profit or commercial advantage and that copies bear this notice and the full citation on the first page. Copyrights for components of this work owned by others than the author(s) must be honored. Abstracting with credit is permitted. To copy otherwise, or republish, to post on servers or to redistribute to lists, requires prior specific permission and/or a fee. Request permissions from permissions@acm.org.

Conference acronym 'XX, Woodstock, NY

© 2018 Copyright held by the owner/author(s). Publication rights licensed to ACM.

ACM ISBN 978-1-4503-XXXX-X/2018/06

<https://doi.org/XXXXXX.XXXXXXX>



Figure 1: An example of heterogeneous retrieval and reranking on a mobile search interface. Given a user query “How to cook cola chicken”, candidate results are recalled from multiple modality-specific queues, including LLM outputs, video content, and natural text.

Therefore, whole-page reranking is both crucial for user experience and technically challenging for SERP.

Existing methods [10–12] for whole-page reranking in search engines typically rely on large-scale human-annotated data. Unlike labeling relevance for individual documents or images, whole-page annotations must evaluate global ranking quality while also accounting for cross-modal relevance differences. Given a user query, annotators not only need to determine the relevance order within the same modality but also assess the relative relevance across different modalities. For example, when a user searches for "How to make Coke Chicken Wings?", it is generally better to rank video results with detailed step-by-step demonstrations higher than dry text descriptions. Therefore, page-level annotations are far more costly and time-consuming than single-modal annotations.

Meanwhile, strong single-modal rankers achieve remarkable performance within their respective domains, such as BERT-based text models [6, 22] and vision-language models [17]. However, naively extending these models to whole-page reranking is nontrivial. Simple fusion methods [15] fail to capture interdependencies among modalities, while naive combinations [20] often lead to suboptimal rankings due to mismatched relevance distributions across modalities. This is because candidates originate from different modalities with distinct schemas and presentation forms, leading to large discrepancies in feature distributions, structural forms, and numeric scales across sources. Figure 2 shows that upstream single-modality

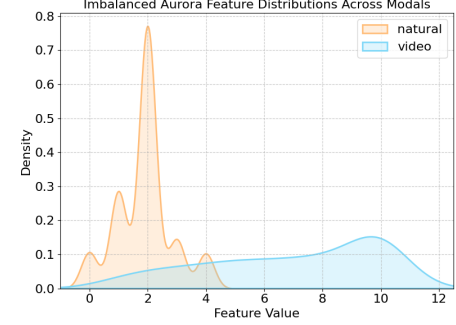


Figure 2: Imbalanced Upstream Model Scores Distributions Across Modals. Upstream model scores is a common feature score computed by the Single-Modal upstream models in Baidu search engine.

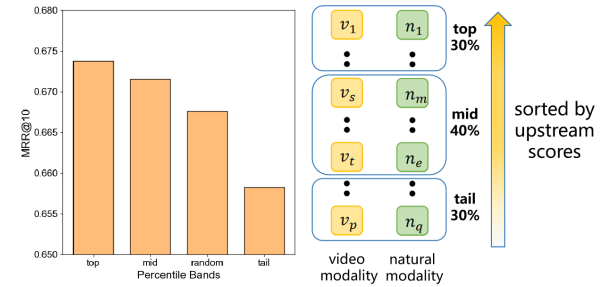


Figure 3: Performance of Percentile bands on Qilin. The video queue and the natural result queue are sorted by upstream model scores. “Random” denotes randomly selecting 30% of the data from each of the two queues.

features for video and natural text results follow markedly different distributions, highlighting the lack of cross-modal comparability. This heterogeneity makes a single global model hard to calibrate under distribution shifts, inflates engineering and labeling overhead, and ultimately constrains both the attainable gains of cross-modality ranking models and the end-user experience on the SERP.

Thus, the key research question becomes: **How can we exploit high-quality single-modal rankers to enhance whole-page reranking while minimizing reliance on costly whole-page annotations?** To this end, we conduct a careful analysis of the annotation quality of single-modal rankers on whole-page reranking data. Specifically, we evaluate the performance of a multimodal reranking model on the Qilin dataset using four groups: a randomly selected 30%, the top 30%, middle 40%, and tail 30% from single-modal rankers, as shown in Figure 3. The results demonstrate that the higher the correlation of the single-modal ranker (i.e., the top group), the better the final multimodal reranking model performs.

In this paper, we propose SMAR, a novel whole-page reranking framework that leverages strong Single-modal rankers to guide Modal-wise relevance Alignment for effective Reranking. Instead of depending solely on costly full-page annotations, SMAR introduces a cross-modal distillation mechanism where single-modal experts provide fine-grained relevance signals to guide the whole-page

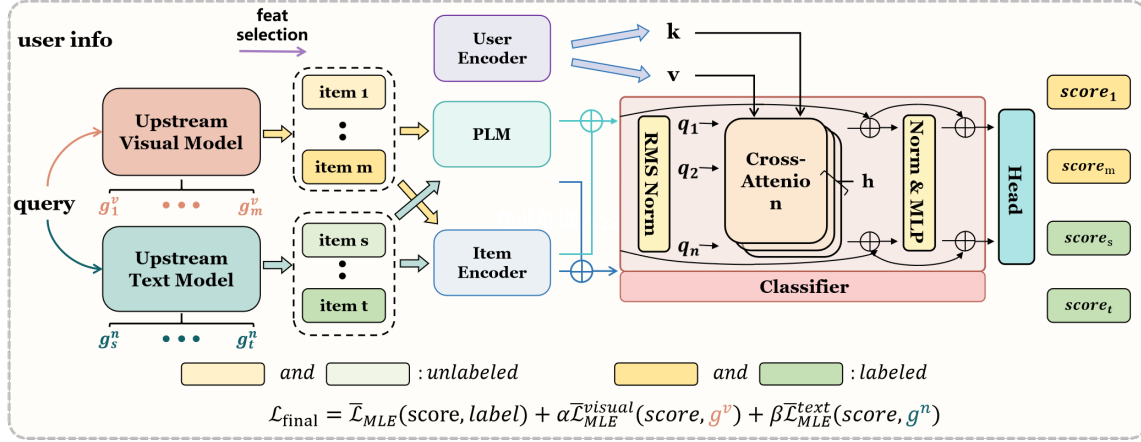


Figure 4: Overall architecture of the proposed user-item interaction model. ① The encoder integrates query semantics with item representations, where a pretrained language model (PLM) encodes query-item textual signals and an item feature extractor incorporates auxiliary item information. ② User-specific features are independently processed by a user feature extractor to produce user embeddings, which are injected into the classifier as keys and values. ③ The classifier employs cross-attention to capture fine-grained interactions between user embeddings and item representations, followed by normalization and multi-layer perceptron (MLP) modules. The head outputs the final relevance scores for candidate items.

reranking model. Specifically, high-quality single-modal rankers are first trained on their modality-specific data. Then, we propose two budget-aware annotation strategies to form candidate pages and perform annotations at the page level: the Top-P strategy and the Iso-label anchors strategy. Top-p annotates only the highest-scoring fraction within each modality while leaving the remainder to weak supervision from upstream scores. Iso-label anchors annotate cross-modal candidates at comparable upstream scores to align preference scales and propagate supervision to the whole-page reranker. Finally, the whole-page reranker is trained using these limited annotations while enforcing consistency with single-modal preferences to preserve intra-modality ranking quality.

Extensive experiments on the Qilin and Baidu datasets demonstrate that SMAR reduces annotation costs by approximately 70–90% while achieving significant improvements over fully annotated reranking baselines. Moreover, both offline evaluations and online A/B testing in Baidu Apps validate the practical effectiveness of SMAR, yielding 0.86% and 0.25% gains in NDCG and CTR as ranking metrics, as well as 1.58% and 0.33% gains in ΔGSB and next-day retained users. These results highlight the promise of aligning single-modal expertise with limited whole-page supervision as a scalable solution for improving SERP quality in real-world search scenarios.¹ Our contributions can be summarized as follows:

- We highlight the annotation bottleneck in whole-page reranking and motivate the need for methods that leverage single-modal rankers to reduce costs.
- We propose two novel modal-wise relevance alignment strategies that distill strong single-modal signals into whole-page reranking by preserving intra-modality preference orderings.

- We conduct extensive experiments on large-scale industrial datasets and real-world platforms, demonstrating that SMAR achieves both annotation efficiency and practical ranking improvements. We also publish an industrial corpus for whole-page reranking research.

2 Model

2.1 Preliminaries

In practical Search Engine systems, candidate items are often retrieved from multiple heterogeneous sources, such as text corpora, multimedia collections, or structured databases. Each source provides a distinct set of candidate items with potentially different feature spaces and relevance distributions. Let \mathcal{U} denote the user space, \mathcal{Q} the query space, and $\{\mathcal{I}^1, \mathcal{I}^2, \dots, \mathcal{I}^M\}$ the candidate item sets retrieved from M heterogeneous sources. Given a user $u \in \mathcal{U}$ and a query $q \in \mathcal{Q}$, the system first performs multimodal retrieval to construct a personalized unified candidate set

$$\mathcal{I} = \bigcup_{m=1}^M \mathcal{I}^m.$$

The goal of personalized heterogeneous ranking is to learn a multimodal scoring function

$$f : \mathcal{U} \times \mathcal{Q} \times \mathcal{I} \rightarrow \mathbb{R},$$

that assigns each item $i \in \mathcal{I}$ a relevance score $s_i = f(u, q, i)$, such that items from different modals can be compared in a shared semantic space and ranked in descending order of relevance:

$$\pi(u, q) = \operatorname{argsort}_{i \in \mathcal{I}} s_i$$

where $\pi(u, q)$ denotes the final ranked list. Although this formulation is conceptually straightforward, learning an accurate scoring function $f(u, q, i)$ is highly non-trivial. The joint space $\mathcal{U} \times \mathcal{Q} \times \mathcal{I}$

¹Our code and data are available at <https://github.com/zzs97str/SMAR>.

is extremely large and high-dimensional. Training a reliable model over this space requires massive amounts of human-labeled data, which is expensive and leads to low efficiency in practice.

2.2 Overall Framework

We leverage upstream single-modal rankers' fine-grained scoring signals for heterogeneous reranking, avoiding large-scale manual annotation. Specifically, the scores assigned to items within a single-modal sequence are transformed into supervision for the multimodal reranking model through pairwise or listwise objectives. This formulation allows us to reuse the strengths of existing rankers, significantly reducing annotation cost while maintaining strong performance in heterogeneous ranking. The overall framework is shown in Figure 4.

2.3 Single-modal Ranker Supervision

Let $\pi^m(q) = \{(i, g_i^m(q)) | i \in \mathcal{I}^m\}$ denote the items and their scores assigned by the upstream single-modal ranker g^m , where $g_i^m(q)$ is the score of item $i \in \mathcal{I}^m$ under query q . These scores serve as supervision signals for training the multimodal reranker $f(u, q, i)$ under two proposed supervision schemes:

Pairwise supervision. Given a query, for any two items $i, j \in \mathcal{I}^m$ from the same source, we define the pairwise preference as:

$$y_{ij} = \mathbb{I}[g_i^m > g_j^m],$$

where $\mathbb{I}[\cdot]$ is the indicator function.

The reranker is trained to preserve this preference by minimizing a pairwise loss:

$$\mathcal{L}_m = y_{ij} \cdot \max(0, \gamma - (f(u, q, i) - f(u, q, j))),$$

where $\gamma > 0$ is the margin hyperparameter.

The total multimodal reranker loss is

$$\mathcal{L}_{pair} = \sum_{m \in \mathcal{M}} \beta_m \cdot \mathcal{L}_m,$$

where β_m is a coefficient of modality m .

Listwise supervision. Alternatively, we can use listwise objectives to train the multimodal reranker. Given a single-modal candidate list \mathcal{I}^m with upstream scores $\{g_i^m\}_{i \in \mathcal{I}^m}$, we normalize them into a probability distribution:

$$p^m(i | q) = \frac{\exp(g_i^m)}{\sum_{j \in \mathcal{I}^m} \exp(g_j^m)}.$$

The reranker then produces a distribution over these candidates:

$$\hat{p}(i | u, q) = \frac{\exp(f(u, q, i))}{\sum_{j \in \mathcal{I}^m} \exp(f(u, q, j))}.$$

The listwise objective minimizes the discrepancy between upstream supervision and the reranker's distribution, e.g., via KL divergence:

$$\mathcal{L}_{list} = D_{KL}(p^m(\cdot | q) \parallel \hat{p}(\cdot | u, q)).$$

If only the ranking order from the upstream model is available while the exact item scores are unknown, one can adopt ListMLE [19], which directly models the permutation likelihood of a ranked list. Given a permutation π sorted by the upstream scores, the ListMLE

loss is defined as:

$$\mathcal{L}_{ListMLE} = - \sum_{k=1}^{|\mathcal{I}^m|} \log \frac{\exp(f(u, q, \pi_k))}{\sum_{j=k}^{|\mathcal{I}^m|} \exp(f(u, q, \pi_j))}.$$

Importantly, the proposed supervision relies solely on relative preferences—that is, whether item A should be ranked above item B—rather than on their absolute scores. For example, the upstream model may only return binned features rather than explicit model prediction scores. In such cases, the multimodal ranking model can still be supervised using pairwise comparisons constructed between items from different bins within a single modality. This design aligns with real-world industrial settings, where information silos across teams or organizations often limit access to raw data.

2.4 Annotation Strategy

Solely training the multimodal reranker models on single-modal data is insufficient. In single-modal ranking, the upstream models, given a query, only consider the relevance between the content of the current modal data and the query. They do not take into account the user's specific modal preferences and which data source is most suitable for the current query. Therefore, effective heterogeneous ranking requires high-quality cross-modal annotations. However, obtaining such high-quality and multimodal annotations is extremely costly. Manual annotation requires substantial human resources, time, and effort, especially when dealing with large-scale and diverse datasets. Instead of annotating the entire dataset, we focus on specific samples that are more representative or have a greater impact on the model's performance. We investigate two annotation strategies: the Top-P strategy and the binary search for iso-label anchors strategy.

2.4.1 Top-P Strategy. Users focus their attention on the first few results and expect to find a satisfactory item among the top entries with minimal effort [5]. Guided by this insight, we adopt a budget-aware annotation policy that prioritizes the highest-exposure region of each source list.

Let \mathcal{M} denote the set of modals. For query q and modal $m \in \mathcal{M}$, an upstream ranker g_m produces a scored list $C_m = \{(x_j, g_m(x_j))\}_{j=1}^{n_m}$. Given a budget ratio $p \in (0, 1]$, we form the labeled pool by taking the top $p \cdot n_m$ items from each C_m . The remaining items are left unlabeled, supervised by their upstream ranker. By selectively annotating these samples, we can improve the model's ability to handle cross-list ranking while keeping the annotation costs under control. This approach allows us to make the most of our limited resources and effectively enhance the performance of the multimodal reranker models in heterogeneous ranking scenarios.

2.4.2 Binary Search for Iso-Label Anchors. Although the feature distributions of different modalities vary for the same query, when the scores produced by upstream single-modality models accurately capture modality-specific preferences, it becomes possible to establish items sharing identical or nearly identical prior satisfaction scores across modalities ("tie") as bridges for alignment. To efficiently identify items with identical prior satisfaction scores while relying on limited labeled data, we employ a Binary Search for Iso-Label Anchors strategy.

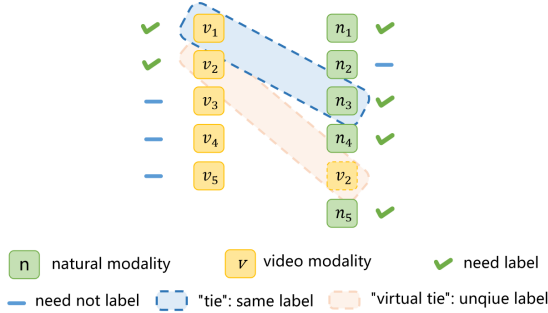


Figure 5: An example of binary search for iso-label anchors. Blue dashed boxes represent tie segments where items share the same label, and orange dashed boxes indicate virtual ties where no item in the natural queue has the same label as v_2 , but natural items with both higher and lower labels exist, leading to the insertion of v_2 as a virtual tie.

Formally, let Q_1 and Q_2 denote two ranked queues, where each queue is sorted by the stable upstream scores. For every $i \in Q_1$, we first label $j \in Q_2$ to check if $\text{label}(Q_1[i]) = \text{label}(Q_2[j])$. If their labels are equal, a “tie” is obtained. Else, we perform a binary search over Q_2 to locate an index j such that $\text{label}(Q_1[i]) = \text{label}(Q_2[j])$. Upon a match, we obtain an equal-label anchor and move on to the next $i' \in Q_1$ to repeat the process until all items are considered in one of the two queues. If all labels in Q_2 are different from $\text{label}(Q_1[i'])$, we insert i' into Q_2 to obtain a “virtual” tie. T denotes the total number of times we search for the ties. The larger the T , the more data we choose. For instance, after searching for 2 times, the results are shown in Figure 5. For labeled items, a pointwise loss is obtained. For n_1 and v_1 , a pairwise loss is obtained, etc. Pseudo-code is provided in Appendix E. Leveraging these anchors, SMAR aligns multimodal label spaces with limited supervision and distills intra-modality preferences from upstream models, enabling effective learning of score distributions across heterogeneous modalities.

2.5 Whole-Page Reranker

A recent study [14] shows self-attention effectively models inter-document importance for context-aware ranking. Yet such methods neglect a key factor in heterogeneous ranking: the user. Preferences and locale shape relevance. For instance, “Java” may mean the Indonesian island for local users but the programming language for many developers, so rerankers should incorporate user features. To address this limitation, our framework introduces a cross-attention module between user embeddings and item embeddings.

As illustrated in Figure 4, the encoder first generates semantic representations of queries and items $\mathbf{e}_i^{\text{sem}}$ using a pretrained language model (PLM). Inspired by [20], we utilize a hybrid fusion to enhance the contribution of $\mathbf{e}_i^{\text{visual}}$ to the final item embedding. Specifically, we first obtain the text embedding $\mathbf{e}_i^{\text{text}}$ from the last token of the final layer output of the VLM, which serves as the comprehensive representation of the textual content. Early fusion maps visual tokens into the VLM’s text space to produce an image-only visual note $\mathbf{e}_i^{\text{visual}}$. In late fusion, we employ a learnable gating mechanism to adaptively combine the visual representation $\mathbf{e}_i^{\text{visual}}$

with the text representation $\mathbf{e}_i^{\text{text}}$, producing the final multimodal embedding:

$$z = \sigma(W[\mathbf{e}_i^{\text{visual}}, \mathbf{e}_i^{\text{text}}] + b), \quad (1)$$

$$\mathbf{e}_i^{\text{sem}} = z \odot \mathbf{e}_i^{\text{visual}} + (1 - z) \odot \mathbf{e}_i^{\text{text}}. \quad (2)$$

Here, σ is the sigmoid function, $[\cdot, \cdot]$ denotes vector concatenation, and \odot is the element-wise product. In parallel, an item feature extractor encodes the numerical and categorical attributes of candidate items into high-dimensional embeddings:

$$\mathbf{e}_i^{\text{feat}} = \text{FFN}(\mathbf{x}_i),$$

where \mathbf{x}_i represents the structured features of item i . Then semantic representations $\mathbf{e}_i^{\text{sem}}$ and item feature embedding $\mathbf{e}_i^{\text{feat}}$ are concatenated into \mathbf{e}_i .

$$\mathbf{e}_i = [\mathbf{e}_i^{\text{sem}}; \mathbf{e}_i^{\text{feat}}],$$

Likewise, a user feature extractor produces user embeddings:

$$\mathbf{e}_u^{\text{user}} = \text{FFN}(\mathbf{x}_u),$$

with \mathbf{x}_u denoting the user features. Both user features \mathbf{x}_u and item features \mathbf{x}_i are bucketized and converted into binary form [13], resulting in a feature vector.

The enriched representations \mathbf{h}_i are processed by a stack of blocks, including normalization, cross-attention mechanisms, multi-layer perceptrons (MLP), and residual connections [8].

$$\mathbf{h}_i = \text{Multi-head CrossAttn}(Q, K, V) \quad (3)$$

$$= \text{Concat}(\text{head}_1, \dots, \text{head}_H)W^O, \quad (4)$$

where each head is computed as

$$\text{head}_j = \text{CrossAttn}\left(W_j^Q \mathbf{e}_i, W_j^K \mathbf{e}_u^{\text{user}}, W_j^V \mathbf{e}_u^{\text{user}}\right).$$

W_Q , W_K , W_V and W^O are learnable projection matrices. H denotes the number of attention heads, which allows the model to jointly capture multiple types of user–item interaction patterns in different subspaces. Finally, the output head produces final ranking scores:

$$s_i = \text{Head}(\text{MLP}(\mathbf{h}_i)).$$

This design enables each candidate item to selectively attend to relevant user signals, thereby yielding interaction-aware representations that jointly capture item relevance and user preference.

During training, we adopt a listwise objective because the Qilin dataset provides only implicit click feedback per item (clicked vs. unclicked) without graded query–item relevance labels. Concretely, we optimize the ListMLE loss. Given model scores $x_q = f_\theta(x_{qj})_{j=1}^{n_q}$ for query q with n_q candidates and a click-derived ordering y_q , following Xia et al. [19]:

$$\mathcal{L}_{\text{MLE}}(x_q, y_q) = -\log(P(y_q | x_q; f)), \quad (5)$$

$$= -\log\left(\prod_{j=1}^{n_q} \frac{\exp(f(x_{qj}))}{\sum_{k=j}^{n_q} \exp(f(x_{qk}))}\right). \quad (6)$$

Throughout this section, the candidate score list x_q is assumed to be ordered according to the target permutation induced by y_q . In practice, we observe that $\mathcal{L}_{\text{MLE}}(x_q, y_q)$ grows with list length, which can destabilize training across queries with heterogeneous candidate sizes. We therefore employ a length-normalized variant:

$$\bar{\mathcal{L}}_{MLE}(x_q, y_q) = \frac{1}{n_q} \mathcal{L}_{MLE}(x_q, y_q) \quad (7)$$

$$= -\frac{1}{n_q} \log \left(\prod_{j=1}^{n_q} \frac{\exp(f(x_{qj}))}{\sum_{k=j}^{n_q} \exp(f(x_{qk}))} \right). \quad (8)$$

Let Q_L and Q_U denote the labeled and unlabeled query sets, respectively. For $q \in Q_L$, we use $\bar{\mathcal{L}}_{MLE}(x_q, y_q)$. For $q \in Q_U$, to inject stable ordering signals from the upstream rankers, we add listwise distillation terms. Let g^v, g^n denote the upstream visual ranker and text ranker, respectively. Accordingly, let $\tilde{y}_q^v = \{g_\theta^v(x_{qj})\}_{j=1}^{n_q}$ and $\tilde{y}_q^n = \{g_\theta^n(x_{qj})\}_{j=1}^{n_q}$ denote the permutations sorted by their output scores. The final objective aggregates both supervision signals over the training set Q :

$$\mathcal{L}_{\text{final}} = \bar{\mathcal{L}}_{MLE}(x_q, y_q) + \alpha \bar{\mathcal{L}}_{MLE}^v(x_q, \tilde{y}_q^v) + \beta \bar{\mathcal{L}}_{MLE}^n(x_q, \tilde{y}_q^n),$$

where α, β balances label supervision and upstream supervisions.

3 Experiments

3.1 Experimental Settings

3.1.1 Dataset. To evaluate our approach, we adopt the public Qilin dataset [4] and Baidu’s DuRank dataset, which are both large-scale industrial datasets for heterogeneous ranking on The Red Book APPs and Baidu APPs, respectively. The detailed process of data is shown in Appendix D.

- **Qilin:** Collected from The Red Book APPs, a large Chinese UGC platform, Qilin comprises more than 15,000 users’ app-level session contexts, 1,900,000 user-generated notes, and 5,000,000 images. It supports two primary tasks, i.e., search and recommendation. With its diverse multimodal content and rich user interactions, Qilin provides a challenging yet realistic benchmark for studying ranking over multimodal heterogeneous data.
- **DuRank:** We publish a high-quality dataset manually annotated by experts. This dataset is collected between May 2024 and March 2025, and contains more than 15,000 user queries, 300,000 retrieved results, and the corresponding human relevance judgments for each query-result pair. The detailed description of this dataset is shown in Appendix B. With its carefully curated annotations and coverage of real user search intents, this dataset serves as a valuable resource for evaluating ranking models in search scenarios. **The DuRank dataset will be publicly released after completing the required anonymization process and upon publication.**

3.1.2 Metrics. We evaluate our reranking methods using three classical ranking metrics for the main experiments, i.e., MRR, MAP, and NDCG. For the offline and online A/B testing, we additionally compare the ranking metrics, such as F1 and PNR, and the user experience metrics, such as IRQ, Next-day Retained User, and ΔGSB . Due to space constraints, detailed descriptions of the Evaluation Metrics are provided in the Appendix A.

3.1.3 Parameter settings. The server is equipped with a Gigabit Ethernet card and utilizes multiple GPUs, including eight NVIDIA A100 and eight NVIDIA V100. FP32 is used to maximize performance for

Method	Labeled Size	Qwen2-VL-2B		
		MRR@10	MAP@10	NDCG
SFT	0%-10% data	0.6269	0.4699	0.4172
SFT	0%-20% data	0.6338	0.4913	0.4428
SFT	0%-30% data	0.6606	0.5016	0.4533
SFT	full data	0.6664	0.5180	0.4693
Only Upstream	-	0.6172	0.4541	0.4038
SMAR	random 30%	0.6676	0.5125	0.4659
SMAR	0%-10%	0.6702	0.5218	0.4756
SMAR	0%-20%	0.6701	0.5184	0.4691
SMAR	0%-30%	0.6738	0.5203	0.4722
SMAR	30%-70%	0.6715	0.5135	0.4670
SMAR	70%-100%	0.6582	0.4647	0.4507
SMAR	full data	0.6687	0.5061	0.4600
SMAR	0%-20%	0.6701	0.5184	0.4691
SMAR	20%-40%	0.6677	0.5023	0.4564
SMAR	40%-60%	0.6676	0.5062	0.4556
SMAR	60%-80%	0.6684	0.4912	0.4433
SMAR	80%-100%	0.6419	0.4805	0.4307

Table 1: Qilin: we test top-p sampling across budgets, where $x\%-y\%$ is the slice of labeled instances by the upstream model’s ranking scores. We fine-tune SMAR on this selected data with human labels plus upstream supervision; the SFT baseline fine-tunes the Reranker only on the top-x% data without single-modal ranker supervision.

Bert-base-chinese and ERNIE (used in the online reranker), while FP16 and lora [9] are used to accelerate the training for Qwen2-VL-2B and Qwen3-Reranker-4B. Other parameter settings are provided in the Appendix C.

3.2 Main Results

3.2.1 Qilin Dataset. To simulate industrial candidate generation, we train two upstream retrieval models on the Qilin dataset by modality: BERT-base-Chinese for text and Qwen-VL-2B for vision-dominant items. Each retriever independently returns a ranked list with relevance scores. The union of these lists forms the multimodal candidate pool and preserves the original upstream ordering as a prior. Under a constrained human and time budget, we leverage the scores generated by upstream single-modality rankers on their respective candidate pools and distill their modality-specific ranking preferences into a unified cross-modality ranking model. The goal is to achieve near full-supervision performance while minimizing the need for expensive and time-consuming annotations.

Experimental results on the Qilin Dataset are shown in Table 1. Using scores from upstream single-modality models for supervision consistently improves the performance of all models trained on the annotated and cross-modality dataset. Moreover, when labeled data are limited, comparing models trained on different quantile segments reveals that annotating only the top-ranked portion of each queue yields better performance than randomly annotating samples or labeling those from the lower-ranked tail. Remarkably, using only the top 10% of annotated data, the proposed SMAR

Method	Labeled Size	Bert-base-chinese [6]			Qwen3-Reranker-4B [22]		
		MRR@1	MRR@2	NDCG	MRR@1	MRR@2	NDCG
SFT	1% data	0.6097	0.7338	0.5762	0.6854	0.7858	0.6332
SFT	3% data	0.6869	0.7873	0.6413	0.7097	0.8007	0.6595
SFT	5% data	0.7078	0.7989	0.6538	0.7213	0.8071	0.6684
SFT	10% data	0.7388	0.8196	0.6840	0.7269	0.8099	0.6710
SFT	20% data	0.7366	0.8160	0.6817	0.7291	0.8142	0.6774
SFT	30% data	0.7418	0.8235	0.6921	0.7377	0.8207	0.6841
SFT	full data	0.7414	0.8218	0.6870	0.7537	0.8308	0.7008
Only Upstream	-	0.7418	0.8248	0.6864	0.7276	0.8170	0.6751
SMAR	1% data	0.7485	0.8285	0.6908	0.7347	0.8183	0.6778
SMAR	3% data	0.7474	0.8269	0.6881	0.7347	0.8198	0.6804
SMAR	5% data	0.7534	0.8317	0.6942	0.7340	0.8160	0.6801
SMAR	10% data	0.7526	0.8326	0.6947	0.7459	0.8224	0.6863
SMAR	20% data	0.7522	0.8338	0.6972	0.7410	0.8224	0.6852
SMAR	30% data	0.7586	0.8340	0.6952	0.7425	0.8256	0.6913
SMAR	full data	0.7448	0.8285	0.6944	0.7559	0.8341	0.7014

Table 2: DuRank: compares retrieval performance across data sizes. The SFT baseline fine-tunes the reranker on a random x% of queries without single-modal ranker supervision. x% of the dataset is treated at the query level, rather than item level.

Method	T_{round}	Labeled Size	F1	NDCG@4	pn
Baseline	-	-	0.7258	0.8766	1.885
Vanilla	-	100%	0.7211	0.8788	2.1527
SMAR-binary search	1	42.09%	0.7134	0.8803	2.0619
SMAR-binary search	2	58.62%	0.7269	0.8791	2.1492
SMAR	-	100%	0.7266	0.8842	2.1342

Table 3: Offline Metrics of Binary Search for Iso-Label Anchors on Baidu APPs.

model surpasses the vanilla model trained on the full annotation set without single-modality supervision across all evaluation metrics.

3.2.2 DuRank Dataset. In the DuRank dataset, upstream signals are derived from independently developed in-house ranking systems. Each query is associated with an average of 4.4 candidate items, which is insufficient for applying the top-p sampling strategy. Therefore, x% of the dataset is treated at the query level. We require at least two natural and two video candidates per query, balance the top-ranked items across modalities as evenly as possible, and discard queries whose maximum relevance score is below 0.8. The BERT-base-chinese is trained with 30 epochs. Due to time constraints, qwen3-reranker is trained with only 15 epochs.

The results of the same experiments on DuRank are shown in the Table 2. Experimental results demonstrate that SMAR remains effective across different model architectures, including the decoder-only Qwen3-Reranker and the encoder-based BERT-Base-Chinese, suggesting the general applicability of our approach. Notably, BERT-Base-Chinese, trained with only 30% of the labeled data, already surpasses its counterpart trained on the full annotation set. In contrast, Qwen3-Reranker exhibits performance gains under single-modality supervision but still falls short of the full annotated data.

Modality	Method	MRR@10	MAP@10	NDCG
text	-	0.5530	0.3969	0.3416
visual	-	0.5776	0.4140	0.3623
multimodal	MLP	0.6021	0.4652	0.4089
multimodal	self-attention [14]	0.6168	0.4785	0.4251
multimodal(SMAR)	cross-attention(w/o hybrid fusion)	0.6633	0.4996	0.4579
multimodal(SMAR)	cross-attention	0.6664	0.5180	0.4693

Table 4: Whole-page reranker with different attention modules on Qilin Dataset. All methods use the hybrid fusion. Training excludes the upstream-ranker supervision.

3.2.3 Binary Search for Iso-label Anchors. The results of binary search for iso-label anchors are shown in Table 3.² When only two rounds of binary search are conducted, SMAR achieves superior performance on both F1 and NDCG while using merely 58.62% of the original dataset. Its PNR score also approaches that of the fully human-annotated supervised model, with a gap of less than 0.01.

3.2.4 Cross-Attention Mechanism. We train the whole-page reranker on the annotated training set to assess the effectiveness of the proposed cross-attention mechanism on the Qilin dataset. The results are reported in Table 4. The rows corresponding to the text and visual modalities represent the performance achieved when models are trained using a single modality on the multimodal ranking task. The experimental results show that the cross-attention architecture incorporating user features significantly outperforms other methods, and the combination of early and late fusion for item representation further amplifies this advantage.

3.3 Online A/B Testing

3.3.1 Settings. Except for the online model, which uses Baidu ERNIE [1], all other whole-page rerankers in this paper are trained

²The iso-label anchor is suitable for discrete bucketed features. Since the model outputs in the Qilin dataset are not bucketed, we conducted this experiment only on DuRank.

with cross-attention and a listwise objective. To fully evaluate the reranking performance of SMAR, we adopt pairwise supervision to distill the upstream single-modal ability into our multimodal relevance model. For each query, results with higher upstream scores are treated as positive samples, while those with lower scores are treated as negative samples. The loss function is

$$\begin{aligned} \text{loss} &= \text{loss}_{\text{pointwise}} + \alpha \cdot \text{loss}_{\text{label pairwise}} + \beta \cdot \text{loss}_{\text{upstream pairwise}} \\ &= \text{loss}(\text{pred}, \text{label}) + \alpha \cdot \max(\text{margin}_1 - (s_{\text{pos}} - s_{\text{neg}}), 0) \\ &\quad + \beta \cdot \max(\text{margin}_2 - (s_{\text{pos}} - s_{\text{neg}}), 0). \end{aligned}$$

The hyperparameters were set as follows: $\text{margin}_1 = 0.1$, $\text{margin}_2 = 0.1$, $\alpha = 0.5$, and $\beta = 0.2$, while s_{pos} and s_{neg} denote the predicted relevance of the positive and negative samples. During the online A/B test, we performed a seven-day experiment (from 2025-09-16 to 2025-10-01) to compare it with our online relevance reranker in a real-world search scenario.

3.3.2 Results. All effects in Figure 6 are reported as relative percentage changes vs. baseline. The treatment increases scale indicators: Search UV (unique users who used search) rises by 0.11% ($p=0.04$), indicating a significant gain; Search PV (search page views) increases by 0.31% ($p=0.24$); and IRQ—the total quantity of results issued, a proxy for search distribution and contributed information—shows a significant 0.48% lift ($p \approx 0.00$). Together with a significant improvement in next-day retention (0.31%, $p=0.01$), these results suggest greater user engagement and perceived relevance. On relevance at different ranks, we analyze the cause of the slight decrease in CTR@1. Through extensive case studies, we observe that the treatment model tends to rank generative answer cards produced by LLMs at the top position. These cards are typically self-contained and satisfy user intent without requiring click-through, which explains the (non-significant) reduction in CTR@1. The treatment boosts mid/tail click propensity, indicating higher-quality ranking beyond the first position and deeper exploration. In addition to CTR@k, aggregated CTR over the top-4 and top-8 increases by 0.16% and 0.25%, respectively. Finally, we observe $\Delta_{\text{GSB}} = 1.58\%$ on randomly sampled queries with 190 effective expert judgements and 0.50% on long-tail queries with 193 effective expert judgements, demonstrating that SMAR outperforms the latest online model under expert human evaluation.

4 Related Work

4.1 Learning to Rank

Learning to Rank (LTR) has been extensively studied in search and recommendation systems, and existing methods generally fall into three paradigms: pointwise, pairwise, and listwise. Pointwise approaches [7] treat ranking as a regression or classification task, predicting each item's relevance independently. Pairwise methods [3, 16] optimize relative preferences by training on positive-negative item pairs, improving discriminative capability. Listwise approaches further consider the entire ranking list, optimizing list-level metrics and modeling item dependencies more effectively. Attention mechanism, as a listwise approach, is designed for explicitly capturing inter-item relationships. Pobrotyn et al. [14] introduced a context-aware listwise model using self-attention to model pairwise interactions within a candidate list. However, such

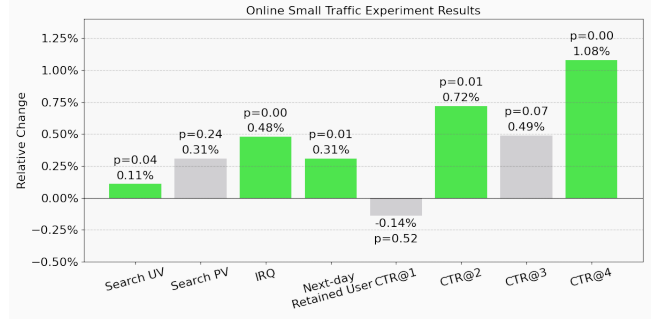


Figure 6: Online A/B test. Bars report the relative change (%) of each metric for the treatment vs. baseline. The y-axis shows a zero-effect baseline. Each bar is annotated with its effect size and p -value. Color encodes statistical significance: green denotes a significant improvement ($p \leq 0.05$ and $\Delta > 0$) and gray denotes a non-significant effect ($p > 0.05$).

models often overlook personalization, assuming uniform user preferences. To address this, we propose Cross-Attention-Rank, which incorporates the user features via cross-attention, aligning user embeddings with item features for personalized ranking.

4.2 Multimodal Ranking

Recent work in multimodal ranking explores integrating visual and textual signals through Multimodal Large Language Models (MLLMs). While these models aim for unified multimodal representations, fine-tuning often favors textual modalities, weakening visual contributions. To mitigate this bias, NoteLLM-2 [20] introduces multimodal in-context learning (mICL) with late fusion, separating visual and textual prompts and applying a gating mechanism to effectively preserve visual information, leading to superior performance in multimodal recommendation. Similarly, the Joint Relevance Estimation (JRE) framework [21] fuses screenshots, HTML, and text of search result pages using inter- and intra-modality attention to balance heterogeneous signals. However, JRE primarily addresses intra-page reranking and does not resolve the scoring misalignment that arises when jointly ranking heterogeneous modality items lacking shared objectives.

5 Conclusion

We introduced SMAR, a whole-page reranking framework that aligns cross-modal relevance by distilling signals from strong single-modal rankers. Rather than relying on expensive page-level labels, SMAR uses Top-P and Iso-label anchors to focus limited annotations, preserving intra-modality order while improving cross-modal ranking ability. Experiments on Qilin and DuRank show that SMAR cuts annotation costs by 70–90% and delivers consistent gains in NDCG, CTR, and downstream engagement in offline evaluations and online A/B tests. These results highlight that coupling single-modal expertise with budget-aware alignment is a practical and scalable path to higher-quality SERP. Future work includes adaptive distillation that responds to intent and distribution shifts, broader modality coverage (e.g., code, agents), and deeper integration with LLM-generated candidates to enhance the user experience.

References

[1] Baidu-ERNIE-Team. 2025. ERNIE 4.5 Technical Report. https://ernie.baidu.com/blog/publication/ERNIE_Technical_Report.pdf.

[2] Gavin Brown, Adam Pocock, Ming-Jie Zhao, and Mikel Luján. 2012. Conditional likelihood maximisation: a unifying framework for information theoretic feature selection. *The journal of machine learning research* 13, 1 (2012), 27–66.

[3] Christopher Burges, Robert Ragno, and Quoc Le. 2006. Learning to rank with nonsmooth cost functions. *Advances in neural information processing systems* 19 (2006).

[4] Jia Chen, Qian Dong, Haitao Li, Xiaohui He, Yan Gao, Shaosheng Cao, Yi Wu, Ping Yang, Chen Xu, Yao Hu, et al. 2025. Qilin: A Multimodal Information Retrieval Dataset with APP-level User Sessions. In *Proceedings of the 48th International ACM SIGIR Conference on Research and Development in Information Retrieval*. 3670–3680.

[5] Aleksandr Chuklin, Ilya Markov, and Maarten De Rijke. 2022. *Click models for web search*. Springer Nature.

[6] Jacob Devlin, Ming-Wei Chang, Kenton Lee, and Kristina Toutanova. 2019. Bert: Pre-training of deep bidirectional transformers for language understanding. In *Proceedings of the 2019 conference of the North American chapter of the association for computational linguistics: human language technologies, volume 1 (long and short papers)*. 4171–4186.

[7] Huifeng Guo, Ruiming Tang, Yuning Ye, Zhenguo Li, and Xiuqiang He. 2017. DeepFM: a factorization-machine based neural network for CTR prediction. *arXiv preprint arXiv:1703.04247* (2017).

[8] Kaiming He, Xiangyu Zhang, Shaoqing Ren, and Jian Sun. 2016. Deep residual learning for image recognition. In *Proceedings of the IEEE conference on computer vision and pattern recognition*. 770–778.

[9] Edward J Hu, Yelong Shen, Phillip Wallis, Zeyuan Allen-Zhu, Yuanzhi Li, Shean Wang, Lu Wang, Weizhu Chen, et al. 2022. Lora: Low-rank adaptation of large language models. *ICLR* 1, 2 (2022), 3.

[10] Canjia Li, Xiaoyang Wang, Dongdong Li, Yiding Liu, Yu Lu, Shuaiqiang Wang, Zhicong Cheng, Simiu Gu, and Dawei Yin. 2023. Pretrained Language Model based Web Search Ranking: From Relevance to Satisfaction. *arXiv preprint arXiv:2306.01599* (2023).

[11] Yuchen Li, Hao Zhang, Haojie Zhang, Hengyi Cai, Xinyu Ma, Shuaiqiang Wang, Haoyi Xiong, Zhaochun Ren, Maarten de Rijke, and Dawei Yin. 2025. Fultr: A large-scale fusion learning to rank dataset and its application for satisfaction-oriented ranking. In *Proceedings of the 31st ACM SIGKDD Conference on Knowledge Discovery and Data Mining* V. 2. 5583–5594.

[12] Haitao Mao, Lixin Zou, Yujia Zheng, Jiliang Tang, Xiaokai Chu, Jiazhao Zhao, Qian Wang, and Dawei Yin. 2024. Whole page unbiased learning to rank. In *Proceedings of the ACM Web Conference 2024*. 1431–1440.

[13] Junwei Pan, Wei Xue, Ximei Wang, Haibin Yu, Xun Liu, Shijie Quan, Xueming Qiu, Dapeng Liu, Lei Xiao, and Jie Jiang. 2024. Ads recommendation in a collapsed and entangled world. In *Proceedings of the 30th ACM SIGKDD Conference on Knowledge Discovery and Data Mining*. 5566–5577.

[14] Przemysław Pobrotny, Tomasz Bartczak, Mikołaj Synowiec, Radosław Bialobrzeski, and Jarosław Bojar. 2020. Context-aware learning to rank with self-attention. *arXiv preprint arXiv:2005.10084* (2020).

[15] Alec Radford, Jong Wook Kim, Chris Hallacy, Aditya Ramesh, Gabriel Goh, Sandhini Agarwal, Girish Sastry, Amanda Askell, Pamela Mishkin, Jack Clark, et al. 2021. Learning transferable visual models from natural language supervision. In *International conference on machine learning*. PMLR, 8748–8763.

[16] Qi Wan, Xiangnan He, Xiang Wang, Jiancan Wu, Wei Guo, and Ruiming Tang. 2022. Cross pairwise ranking for unbiased item recommendation. In *Proceedings of the ACM web conference 2022*. 2370–2378.

[17] Peng Wang, Shuai Bai, Sinan Tan, Shijie Wang, Zhihao Fan, Jinze Bai, Kepin Chen, Xuejing Liu, Jialin Wang, Wenbin Ge, Yang Fan, Kai Dang, Mengfei Du, Xuancheng Ren, Rui Men, Dayiheng Liu, Chang Zhou, Jingren Zhou, and Junyang Lin. 2024. Qwen2-VL: Enhancing Vision-Language Model's Perception of the World at Any Resolution. *arXiv preprint arXiv:2409.12191* (2024).

[18] Yue Wang, Dawei Yin, Luo Jie, Pengyuan Wang, Makoto Yamada, Yi Chang, and Qiaozhu Mei. 2016. Beyond ranking: Optimizing whole-page presentation. In *Proceedings of the Ninth ACM International Conference on Web Search and Data Mining*. 103–112.

[19] Fen Xia, Tie-Yan Liu, Jue Wang, Wensheng Zhang, and Hang Li. 2008. Listwise approach to learning to rank: theory and algorithm. In *Proceedings of the 25th international conference on Machine learning*. 1192–1199.

[20] Chao Zhang, Haixin Zhang, Shiwei Wu, Di Wu, Tong Xu, Xiangyu Zhao, Yan Gao, Yao Hu, and Enhong Chen. 2025. Notellm-2: Multimodal large representation models for recommendation. In *Proceedings of the 31st ACM SIGKDD Conference on Knowledge Discovery and Data Mining* V. 1. 2815–2826.

[21] Junqi Zhang, Yiqui Liu, Shaoping Ma, and Qi Tian. 2018. Relevance estimation with multiple information sources on search engine result pages. In *Proceedings of the 27th ACM International Conference on Information and Knowledge Management*. 627–636.

[22] Yanzhao Zhang, Mingxin Li, Dingkun Long, Xin Zhang, Huan Lin, Baosong Yang, Pengjun Xie, An Yang, Dayiheng Liu, Junyang Lin, Fei Huang, and Jingren Zhou. 2025. Qwen3 Embedding: Advancing Text Embedding and Reranking Through Foundation Models. *arXiv preprint arXiv:2506.05176* (2025).

A Metrics

A.1 Offline Metrics

- **MRR@k** (Mean Reciprocal Rank)

MRR@k measures how well the model ranks the *first relevant result* at a high position. Higher MRR indicates that users can find relevant items earlier. For a set of queries Q , let rank_i denote the rank position of the first relevant item for query q_i . Then

$$\text{MRR}@k = \frac{1}{|Q|} \sum_{i=1}^{|Q|} \frac{\mathbb{I}(\text{rank}_i \leq k)}{\text{rank}_i},$$

where $\mathbb{I}(\cdot)$ is the indicator function.

- **MAP@k** (Mean Average Precision)

MAP@k measures the model's ability to rank *all relevant items* higher, not just the first one. Higher MAP indicates better ranking consistency across relevant results. For query q_i ,

$$P_i@j = \frac{1}{j} \sum_{t=1}^j \text{rel}_i(t).$$

where,

$$\text{rel}_i(t) = \begin{cases} 1, & \text{if item at rank } t \text{ is relevant,} \\ 0, & \text{otherwise.} \end{cases}$$

The average precision at cutoff k is

$$AP_i@k = \frac{1}{R_i} \sum_{j=1}^k P_i(j) \cdot \text{rel}_i(j),$$

where $R_i = \sum_{j=1}^k \text{rel}_i(j)$. The mean average precision is

$$\text{MAP}@k = \frac{1}{|Q|} \sum_{i=1}^{|Q|} AP_i@k.$$

- **NDCG** (Normalized Discounted Cumulative Gain)

NDCG measures the ability of the model to rank highly relevant items near the top, with emphasis on both position and graded relevance. For query q_i , the discounted cumulative gain is:

$$DCG_i = \sum_{j=1}^N \frac{2^{\text{rel}_i(j)} - 1}{\log_2(j+1)}$$

where N is the number of retrieved items for query q_i and $\text{rel}_i(j)$ is the graded relevance of the item at rank j . The ideal DCG (IDCG) is computed by sorting items by true relevance. Then

$$\text{NDCG} = \frac{1}{|Q|} \sum_{i=1}^{|Q|} \frac{DCG_i}{IDCG_i}$$

- **F1** (Harmonic Mean of Precision and Recall)

F1 evaluates the balance between precision and recall without relying on a cutoff. For query q_i , let S_i be the set of items returned by the system (e.g., the full ranked list or those

above a fixed decision threshold), and let \mathcal{R}_i be the set of ground-truth relevant items with $r_i = |\mathcal{R}_i|$. Define

$$P_i = \begin{cases} \frac{|\mathcal{S}_i \cap \mathcal{R}_i|}{|\mathcal{S}_i|}, & |\mathcal{S}_i| > 0, \\ 0, & \text{otherwise,} \end{cases} \quad R_i = \frac{|\mathcal{S}_i \cap \mathcal{R}_i|}{r_i}.$$

The per-query F1 score is

$$F1_i = \begin{cases} \frac{2P_iR_i}{P_i + R_i}, & P_i + R_i > 0, \\ 0, & \text{otherwise.} \end{cases}$$

We report the macro-average over queries with at least one relevant item:

$$F1 = \frac{1}{|Q'|} \sum_{i \in Q'} F1_i, \quad Q' = \{i \mid r_i > 0\}.$$

- **PNR (Positive–Negative Ratio)**

PNR quantifies pairwise order consistency between model scores and ground-truth relevance. For query q_i with candidates indexed by $a \in \{1, \dots, n_i\}$, let $y_{i,a}$ denote the ground-truth relevance (larger is more relevant) and $s_{i,a}$ the model score. Define the counts of concordant and discordant labeled pairs as

$$C_i = \sum_{a=1}^{n_i} \sum_{b=1}^{n_i} \mathbb{I}(y_{i,a} > y_{i,b}) \mathbb{I}(s_{i,a} > s_{i,b}), \quad (9)$$

$$D_i = \sum_{a=1}^{n_i} \sum_{b=1}^{n_i} \mathbb{I}(y_{i,a} > y_{i,b}) \mathbb{I}(s_{i,a} < s_{i,b}). \quad (10)$$

Label ties are excluded by construction; score ties are ignored. Then

$$\text{PNR}_i = \frac{C_i}{D_i},$$

and the dataset-level metric is the macro-average

$$\text{PNR} = \frac{1}{|Q|} \sum_{i=1}^{|Q|} \text{PNR}_i.$$

Higher PNR indicates fewer pairwise inversions and stronger alignment with ground truth.

A.2 Online Metrics

Search UV counts the number of unique users who interacted with the search surface. **Search PV** counts the number of search page views. **Issued Result Quantity (IRQ)** is the number of results delivered to users and subsequently viewed. It is a key indicator of search scale and, to some extent, quantifies the amount of information contributed by the search engine. **Next-day Retained User** refers to the fraction of users who return the following day. For click metrics, **CTR@k** denotes the position-specific click-through rate at rank position k (clicks on position k divided by impressions of position k), for $k \in \{1, 2, 3, 4\}$. Relative to the online baseline, we obtain N expert pairwise judgments. Letting $\#good$ and $\#bad$ denote counts favoring our model vs. baseline, we define

$$\Delta\text{GSB} = \frac{\#good - \#bad}{2 \times (\#good + \#bad + \#same)}.$$

Positive ΔGSB indicates a net human preference for our model.

B DuRank Dataset

The DuRank dataset was constructed from real user interactions on the Baidu App. It contains query data and high-quality annotations obtained through expert labeling. The dataset primarily consists of search results retrieved from Baidu's natural ranking channel and video ranking channel, with more than 200,000 video results and 40,000 natural results included. Each sample contains a query, the corresponding retrieved results with titles, summaries, categorizations, upstream model scores, and human-annotated relevance, etc. The DuRank dataset comprises single-modality and multi-modality corpora. The single-modality corpus provides only a training set, where all results for a given query come from the same source, either natural search results or video results, and each query is paired with at least two results. The multi-modality corpus includes both training and test sets, and each query is associated with at least two results drawn from different modalities. Expert-annotated relevance is provided on a five-point scale ranging from 0 to 4, indicating the degree to which an item satisfies the user query. A score of 0.0 denotes that the item fails to meet the query at all, while a score of 4.0 denotes that the item fully satisfies the query. Owing to its high-quality human annotations, the Durank dataset enables search engines to better capture the relevance between user queries and retrieved results, thereby providing a valuable dataset for multimodal ranking research.

C Parameter settings

In the Qlin experiments, we train for 30 epochs with a batch size of 1 at the query level, where each query contains multiple candidate items whose total number corresponds to the actual model input batch size. The maximum sequence length is set to 512, which is sufficient for nearly all items, and the learning rate is 1×10^{-5} .

In the DuRank experiments, for the Qwen3-Reranker model, we train for 15 epochs with a learning rate of 2×10^{-6} and a batch size of 2, applying LoRA fine-tuning to both attention and MLP layers within the attention blocks. For the BERT-Base-Chinese model, we train for 30 epochs with a batch size of 32, a maximum sequence length of 512, and a learning rate of 1×10^{-5} .

D Data Processing

To facilitate both single-modality and mixed-modality ranking experiments, we reorganize the original Qlin dataset into dedicated training and test sets, ensuring that evaluation metrics reflect realistic ranking scenarios. In particular, we enforce that, for each query in the test set, the number of non-clicked items exceeds the number of clicked items, ideally by a factor of three. This design prevents artificially inflated MRR scores that could arise if all candidate items under a query are clicked.

For single-modality data, we split the training set according to text and image modalities. For textual data, each candidate document for a given query is first scored by QwenReranker using the concatenated query-document input. Among the clicked items, those with a Qwen3 reranker similarity score below 0.1 are treated as image-driven clicks and are excluded from the textual training set. The threshold 0.1 is set manually after careful inspection. Conversely, clicked items with a score above 0.1 are retained as positive samples. Non-clicked items, regardless of modality, are included as

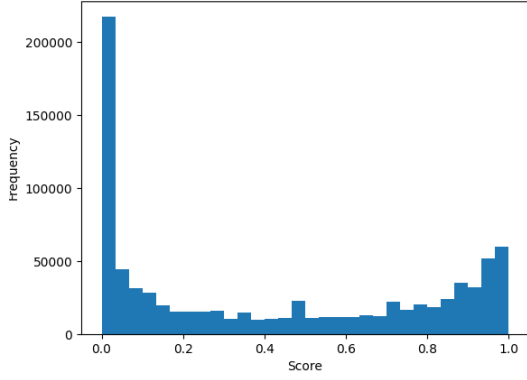


Figure 7: Distribution of QwenReranker scores for candidate items in the Qilin dataset. Scores are used to distinguish text-driven and image-driven clicks.

Algorithm 1 Binary search for iso-label anchors

Input: Two modality queues Q_1 (video) and Q_2 (natural), sorted by upstream scores; maximum rounds T_{rounds}
Output: Cross-modality sequence S containing tie, virtual_tie, and single segments.

```

1: Initialize  $S \leftarrow []$ , and search index  $i \leftarrow 0$  in  $Q_1$ 
2: for  $i = 1$  to  $|Q_1|$  do
3:    $a \leftarrow Q_1[i]$ 
4:    $k \leftarrow \text{BinarySearch}$  in  $Q_2$  for item with  $Q_2[k].label = a.label$ 
5:   if  $k$  found then
6:     Append tie( $a, Q_2[k]$ ) to  $S$ 
7:      $T_{\text{rounds}} += 1$ 
8:   else if there exist higher and lower labels around  $a.label$  in  $Q_2$  then
9:     Append virtual_tie( $a, a^{(\text{virtual})}$ ) to  $S$ 
10:     $T_{\text{rounds}} += 1$ 
11:   else if all labels in  $Q_2[j:] > a.label$  then
12:     Append concatenate( $Q_2[j:], a$ ) as single to  $S$ 
13:   else if all labels in  $Q_2[j:] < a.label$  then
14:     Append concatenate( $a, Q_2[j:]$ ) as single to  $S$ 
15:   end if
16:   if rounds exceed  $T_{\text{rounds}}$  then
17:     Append remaining items as single segments; break
18:   end if
19: end for
20: return  $S$ 

```

negative samples, forming a balanced training set for text ranking. For image-based ranking, since user clicks are naturally driven by both images and titles, we retain the original dataset without further filtering. These two datasets are independent for training models of different modalities.

The test set is processed in a similar fashion. For text ranking, clicked items with a low Qwen score are considered image-driven and their click label is set to 0, while clicked items with a high score

Algorithm 2 Pair construction based on iso-label anchors

Input: Aligned sequence S with optional labels or aurora scores
Output: Pair set \mathcal{P} for pairwise supervision, and pointwise set \mathcal{P}^0

```

1:  $\mathcal{P} \leftarrow \emptyset, \mathcal{P}^0 \leftarrow \emptyset$ 
2: for all pairs  $(x, y)$  within or across queues in  $S$  do
3:   if  $x$  and  $y$  have labels then
4:     if  $x.label > y.label$  then
5:        $\mathcal{P} \leftarrow \mathcal{P} \cup \{(x, y)\}$ 
6:     else
7:        $\mathcal{P} \leftarrow \mathcal{P} \cup \{(y, x)\}$ 
8:     end if
9:   else if labels unavailable and  $x, y$  from same queue then
10:    if  $x.aurora > y.aurora$  then
11:       $\mathcal{P} \leftarrow \mathcal{P} \cup \{(x, y)\}$ 
12:    else
13:       $\mathcal{P} \leftarrow \mathcal{P} \cup \{(y, x)\}$ 
14:    end if
15:   end if
16: end for
17: for all item  $x$  with known label do                                 $\triangleright$  pointwise supervision
18:    $\mathcal{P}^0 \leftarrow \mathcal{P}^0 \cup \{(x, x)\}$ 
19: end for
20: return  $(\mathcal{P}, \mathcal{P}^0)$ 

```

retain a click label of 1. Non-clicked items are consistently labeled as 0. Image-based test data remain unchanged, as user interactions already reflect the joint effect of images and titles. For listwise objection, all candidate items are further sorted according to Wilson-smoothed click-through rates.

For mixed-modality ranking, we distinguish the modality of candidate items for each query. Clicked items with low textual relevance are treated as image-driven, while high textual scores are assumed to text-driven, though potential image contributions are ignored. The ranking objective in this setting is to ensure that clicked items are placed above non-clicked ones, allowing the model to learn to integrate signals across modalities effectively.

Figure 7 presents the distribution of QwenReranker scores across candidate items, illustrating the separation between text- and image-driven clicks and providing guidance for subsequent model training and evaluation.

For the text modality, we concatenate each item’s title and content as its textual representation. For the visual modality, the image title is incorporated into the visual-language model (VLM) prompt, while the image itself is used as input to the ViT component of Qwen-VLM.

D.1 Feature Selection via Entropy-Based Sorting

To mitigate the high cost of manual annotation while preserving discriminative features, we employ entropy-based sorting for numerical feature selection [2]. The entropy $H(X)$ of each feature X is calculated to quantify its information content, with features ranked in descending order of entropy. This ensures that features with higher information gain (e.g., aurora scoring from upstream models) are prioritized over redundant ones (e.g., howto). The final

selected numerical features include QUERY_SEARCH, SCS_ERNIE, aurora, CLICK_SKIP_RATIO, and others as listed in Table 1, while categorical features like is_wenda are encoded as binary indicators.

For the cross-modality ranking model in Qilin, we align aurora score sequences with human-annotated 5-point labels (0-4) to minimize the discrepancy between predicted and true rankings. The dataset is partitioned into training (70%), validation (15%), and test (15%) sets, ensuring sufficient candidate diversity to compute robust metrics like MRR and NDCG.

E Binary Search for Iso-Label Anchors

Algorithm 1 employs a binary search strategy to locate items with identical relevance labels across different modalities. Then in algorithm 2, the limited amount of labeled data serves as pointwise supervision, guiding the cross-modality ranking model to predict accurate prior relevance scores for items. For unlabeled data, items are distinguished according to the modality-specific scores produced by the respective upstream single-modality models.